J|A|C|S
ARTICLES
Published on Web 03/20/2007

# A Density Functional Study of the $^{13}C$ NMR Chemical Shifts in Functionalized Single-Walled Carbon Nanotubes

Eva Zurek,*,† Chris J. Pickard,‡ and Jochen Autschbach*,¶

*Contribution from the Max-Planck-Institut für Festkörperforschung, Heisenbergstrasse1, 70569 Stuttgart, Germany, School of Physics & Astronomy, University of St. Andrews, North Haugh, St. Andrews KY16 9SS, Scotland, and Department of Chemistry, State University of New York at Buffalo, Buffalo, New York 14260-3000*

Received December 19, 2006; E-mail: jochena@buffalo.edu

***Abstract:*** The $^{13}C$ NMR chemical shifts for functionalized (7,0), (8,0), (9,0), and (10,0) single-walled carbon nanotubes (SWNTs) have been studied computationally using gauge-including projector-augmented plane-wave (GIPAW) density functional theory (DFT). The functional groups NH, $NCH_3$, $NCH_2OH$, and $CH_2$-$NHCH_2$ have been considered, and different sites where covalent addition or substitution may occur have been examined. The shifts of the carbons directly attached to the group are sensitive to the bond which has been functionalized and may, therefore, be used to identify whether the group has reacted with a parallel or a diagonal C−C bond. The addition of NH to a parallel bond renders the functionalized carbons formally $sp^3$-hybridized, yielding shifts of around 44 ppm, independent of the SWNT radius. Reaction with a diagonal bond retains the formal $sp^2$ hybridization of the substituted carbons, and their shifts are slightly lower or higher than those of the unsubstituted carbon atoms. The calculated $^1H$ NMR shifts of protons in the functional groups are also dependent upon the SWNT−group interaction. Upon decreasing the degree of functionalization for the systems where the group is added to a parallel bond, the average chemical shift of the unfunctionalized carbons approaches that of the pristine tube. At the same time, the shifts of the functionalized carbons remain independent upon the degree of functionalization. For the SWNTs where N−R attaches to a parallel bond, the average shift of the $sp^2$ carbons was found to be insensitive to the substituent R. Moreover, the shifts of the functionalized $sp^3$ carbons, as well as of the carbons within the group itself, are independent of the SWNT radius. The results indicate that a wealth of knowledge may be obtained from the $^{13}C$ NMR of functionalized SWNTs.

## 1. Introduction

The properties, separation, and potential applications of carbon nanotubes[1] are currently under intense study. The wide range of proposed applications[2] (e.g., in Schottky diodes,[3] as electron field emitters,[4] artificial muscles,[5] magnetic tips for magnetic scanning probe microscopy,[6] or as gas,[7] DNA,[8] and protein[9] sensors) stems from the fact that carbon nanotubes have a diverse range of weights, electronic structures, helicities, etc. A SWNT can conceptually be constructed from the rolling of a graphene sheet. Its structure is conveniently classified by a pair of numbers ($n$,$m$) indexing the two carbons that coincide upon rolling. The separation of these carbons on the planar graphene sheet is $n\mathbf{a}_1 + m\mathbf{a}_2$, where $\mathbf{a}_1$ and $\mathbf{a}_2$ are the unit vectors of the two-dimensional hexagonal graphene lattice. This results in three classes of SWNTs, armchair, zigzag, and helical (chiral), characterized by ($n$,$n$), ($n$,0), and ($n$,$m$) with $n \neq m$, respectively. Noncovalent and covalent functionalization of the tubes can render them soluble in aqueous media and, therefore, potentially useful in biotechnology and biomedical applications.[10,11] For example, such systems show promise as gene-transfer vector systems[12] and in drug delivery.[13]

Unfortunately, it is difficult to fully characterize a given (heterogeneous) sample of nanotubes.[2] Furthermore, the SWNT−functional group interaction is not well understood. For example,

† Max-Planck-Institut für Festkörperforschung.
‡ University of St. Andrews.
¶ State University of New York at Buffalo.

(1) Iijima, S. *Nature* **1991**, *354*, 56−58.
(2) Minett, A.; Atkinson, K.; Roth, S. Carbon Nanotubes. In *Handbook of Porous Solids*; Schüth, F., Sing, S. W., Weitkapmp, J., Eds.; Wiley-VCH: Weinheim, Germany, 2002.
(3) Manohara, H. M.; Wong, E. W.; Schlecht, E.; Hunt, B. D.; Siegel, P. H. *Nano Lett.* **2005**, *5*, 1469−1474.
(4) Zhou, O.; Shimoda, H.; Gao, B.; Oh, S. J.; Fleming, L.; Yue, G. Z. *Acc. Chem. Res.* **2002**, *35*, 1045−1053.
(5) Baughman, R. H.; Cui, C. X.; Zakhidov, A. A.; Iqbal, Z.; Barisci, J. N.; Spinks, G. M.; Wallace, G. G.; Mazzoldi, A.; De Rossi, D.; Rinzler, A. G.; Jaschinski, O.; Roth, S.; Kertesz, M. *Science* **1999**, *284*, 1340−1344.
(6) Kim, Y.-H.; Choi, J.; Chang, K. J.; Tománek, D. *Phys. Rev. B* **2003**, *68*, 125420-1−125420-4.
(7) Snow, E. S.; Perkins, F. K.; Houser, E. J.; Badescu, S. C.; Reinecke, T. L. *Science* **2005**, *307*, 1942−1945.
(8) Tang, X. W.; Bansaruntip, S.; Nakayama, N.; Yenilmez, E.; Chang, Y.-L.; Wang, Q. *Nano Lett.* **2006**, *6*, 1632−1636.
(9) Chen, R. J.; Choi, H. C.; Bangsaruntip, S.; Yenilmez, E.; Tang, X. W.; Wang, Q.; Chang, Y.-L.; Dai, H. J. *J. Am. Chem. Soc.* **2004**, *126*, 1563−1568.
(10) Lin, Y.; Taylor, S.; Li, H. P.; Fernando, K. A. S.; Qu, L. W.; Wang, W.; Gu, L. R.; Zhou, B.; Sun, Y.-P. *J. Mater. Chem.* **2004**, *14*, 527−541.
(11) Tasis, D.; Tagmatarchis, N.; Bianco, A.; Prato, M. *Chem. Rev.* **2006**, *106*, 1105−1136.
(12) Singh, R.; Pantarotto, D.; McCarthy, D.; Chaloin, O.; Hoebeke, J.; Partidos, C. D.; Briand, J.-P.; Prato, M.; Bianco, A.; Kostarelos, K. *J. Am. Chem. Soc.* **2005**, *127*, 4388−4396.
(13) Bianco, A.; Kostarelos, K.; Prato, M. *Curr. Opin. Chem. Biol.* **2005**, *9*, 674−679.


**10.1021/ja069110h CCC: $37.00** 

even though the structures of fluorinated nanotubes have been theoretically and experimentally investigated, a consensus about the most likely bonding pattern has not yet been reached.[11] Periodic[14] and finite-fragment[15] DFT calculations have shown that functional groups such as $CCl_2$, $NCOOC_2H_5$, $CH_2$, NH, $SiH_2$, and O prefer to attach to the bond diagonal to the tube axis of a zigzag nanotube, whereas other solid-state computations have found that structures where a $CCl_2$ group is attached to the bond parallel to the tube axis are slightly lower in energy.[16] For armchair tubes, the computations all suggest that addition of the functional group to a bond perpendicular to the tube axis is preferred, resulting in the sidewall opening of the SWNT.[14,16,17] For both (*n*,0) and (*n*,*n*) tubes, the energy difference between possible isomers was found to decrease as the diameter of the tube increased,[16,17] which has led to the conclusion that, in a sample with typical SWNT diameters, there is no particularly strong site preference for the bonding of the functional group.[16] Since the band structure is dependent upon the degree and position of functionalization,[14,16,18] it is important to be able to determine experimentally how the functional groups interact with the SWNTs, for example, in order to perform effective band-gap engineering.

In chemistry, one of the most versatile experimental tools to study the geometry and electronic structure of molecules and solids is nuclear magnetic resonance (NMR). So far, NMR has not been among the main tools for the characterization of carbon nanostructures. However, recently, the field has started to bloom, and an increasing amount of experimental and theoretical research is becoming available. MAS−NMR measurements on pristine nanotubes have identified isotropic shifts of 124,[19] 116,[20] and 126 ppm[21,22]. Samples with a low metal content and few defects have resulted in resonances of 125,[23] 124,[24] and 121 ppm[25] with line widths of only 9−10 ppm. In all cases, the sample composition was not determined, and therefore, it is unclear if the differences in the shifts arise from a different diameter distribution,[26,27] semiconducting to metallic ratio,[28] or increased concentration of the small band-gap (9,0), (12,0), and (15,0) species.[27] NMR studies of carbon nanohorn aggregates suggest that these systems are composed of two components, yielding shifts of 124 and 116 ppm.[29] The former has been ascribed to a nanotube-like horn, whereas the latter was thought to indicate the presence of a graphite-like species.

In the past few years, $^{13}C$ MAS−NMR studies on functionalized SWNTs have also begun to appear. A sample of shortened pristine tubes ($\delta = 125$ ppm) yielded a spectrum with significant line broadening and the appearance of a strong shoulder at ∼160 ppm, indicating, respectively, the presence of defects and the formation of carbonyl groups at the ends of the species.[23] Upon functionalization with phenol, the chemical shifts of the shortened SWNTs lowered slightly to about 120 ppm. Two-dimensional $^1H-^{13}C$ heteronuclear correlation spectroscopy of these systems yielded evidence of significant nanotube−functional group interaction. The change of the SWNT resonances to a slightly lower shift of ∼118 ppm was attributed to a change in hybridization, from $sp^2$ to $sp^3$, upon functionalization. Other studies showed that functionalization with $(CH_2)_n$-COOH ($n = 2, 3$) resulted in the broadening of the NMR spectrum and shifted the peak maximum from 124 to 121−122 ppm.[24] Functionalization with $CH_2CH_2CONHCH_2CH_2NH_2$ also yielded a peak at 121 ppm but had very little effect on the line width of the sample. Signals from the carbonyl ($\delta = 172$ ppm) and amide ($\delta = 174$ ppm) groups were detected as well. In both of these studies, the resonances of the functionalized tubes were slightly lower in frequency than those of the pristine ones. However, protonation of a sample of SWNTs yielded peaks at 128 and 125 ppm, respectively, as compared to a shift of 121 ppm for the pristine species.[25] It is unclear if the different behavior of the chemical shifts upon functionalization is a result of varying the functional groups or of the introduction of carbonyl groups at the tube ends via the shortening procedure. For example, computations have indicated that the shifts of the central carbon atoms in hydrogen-capped and $C_{30}$-capped finite SWNT fragments might not converge to the same value.[30] Recent experiments have illustrated that it is also possible to measure solution $^{13}C$ NMR of SWNTs.[31] In particular, diamine-terminated oligomeric poly(ethylene glycol) ($PEG_{1500N}$)-functionalized SWNTs yielded a broad signal exhibiting a shoulder which could be deconvoluted into a large and small peak centered around 128 and 144 ppm, respectively. On the basis of theoretical estimates,[28,30] the former was tentatively assigned to semiconducting and the latter to metallic SWNTs. The breadth of the individual peaks was attributed to the presence of tubes with differing diameters and helicities. A solid-state MAS spectrum yielded a double peak (128 and 136 ppm) instead, with the same tentative assignment. $^1H$ NMR has also been used to characterize functionalized SWNTs. The signals obtained are typically broad and weak, especially for protons in proximity to the tube wall, resulting in uncertainties of a few parts per million (ref 32 and references within).

On the theoretical side, it was suggested that metallic and semiconducting SWNTs should be clearly distinguishable by $^{13}C$ NMR because of a predicted 11−12 ppm difference in their

(14) Zhao, J. J.; Chen, Z. F.; Zhou, Z.; Park, H.; Schleyer, P. v. R.; Lu, J. P. *ChemPhysChem* **2005**, *6*, 598−601.
(15) Chen, Z. F.; Nagase, S.; Hirsch, A.; Haddon, R. C.; Thiel, W.; Schleyer, P. v. R. *Angew. Chem., Int. Ed.* **2004**, *43*, 1552−1554.
(16) Cho, E.; Kim, H.; Kim, C.; Han, S. *Chem. Phys. Lett.* **2006**, *419*, 134−138.
(17) Lee, Y.-S.; Marzari, N. *Phys. Rev. Lett.* **2006**, *97*, 116801-1−116801-4.
(18) Lu, J.; Wang, D.; Nagase, S.; Ni, M.; Zhang, X. W.; Maeda, Y.; Wakahara, T.; Nakahodo, T.; Tsuchiya, T.; Akasaka, T.; Gao, Z. X.; Yu, D. P.; Ye, H. Q.; Zhou, Y. S.; Meit, W. N. *J. Phys. Chem. B* **2006**, *110*, 5655−5658.
(19) Tang, X.-P.; Kleinhammes, A.; Shimoda, H.; Fleming, L.; Bennoune, K. Y.; Shina, S.; Bower, C.; Zhou, O.; Wu, Y. *Science* **2000**, *288*, 492−494.
(20) Hayashi, S.; Hoshi, F.; Ishikura, T.; Yumura, M.; Ohshima, S. *Carbon* **2003**, *41*, 3047−3056.
(21) Bac, C. G.; Latil, S.; Vaccarini, L.; Bernier, P.; Gaveau, P.; Tahir, S.; Micholet, V.; Aznar, R.; Rubio, A.; Metenier, K.; Bequin, F. *Phys. Rev. B* **2001**, *63*, 100302-1−100302-4.
(22) Goze-Bac, C.; Latil, S.; Lauginie, P.; Jourdain, V.; Conard, J.; Duclaux, L.; Rubio, A.; Bernier, P. *Carbon* **2002**, *40*, 1825−1842.
(23) Cahill, L. S.; Yao, Z.; Adronov, A.; Penner, J.; Moonoosawmy, K. R.; Kruse, P.; Goward, G. R. *J. Phys. Chem. B* **2004**, *108*, 11412−11418.
(24) Peng, H. Q.; Alemany, L. B.; Margrave, J. L.; Khabashesku, V. N. *J. Am. Chem. Soc.* **2003**, *125*, 15174−15182.
(25) Engtrakul, C.; Davis, M. F.; Gennett, T.; Dillon, A. C.; Jones, K. M.; Heben, M. J. *J. Am. Chem. Soc.* **2005**, *127*, 17548−17555.
(26) Marques, M. A. L.; d'Avezac, M.; Mauri, F. *Phys. Rev. B* **2006**, *73*, 125433-1−125433-6.
(27) Zurek, E.; Pickard, C. J.; Walczak, B.; Autschbach, J. *J. Phys. Chem. A* **2006**, *110*, 11995−12004.
(28) Latil, S.; Henrard, L.; Bac, C. G.; Bernier, P.; Rubio, A. *Phys. Rev. Lett.* **2001**, *86*, 3160−3163.
(29) Imai, H.; Babu, P. K.; Oldfield, E.; Wieckowski, A.; Kasuya, D.; Azami, T.; Shimakawa, Y.; Yudasaka, M.; Kubo, Y.; Iijima, S. *Phys. Rev. B* **2006**, *73*, 125405-1−125405-7.
(30) Zurek, E.; Autschbach, J. *J. Am. Chem. Soc.* **2004**, *126*, 13079−13088.
(31) Kitaygorodskiy, A.; Wang, W.; Xie, S.-Y.; Lin, Y.; Fernando, K. A. S.; Wang, X.; Qu, L. W.; Chen, B.; Sun, Y.-P. *J. Am. Chem. Soc.* **2005**, *127*, 7517−7520.
(32) D'Este, M.; De Nardi, M.; Menna, E. *Eur. J. Org. Chem.* **2006**, 2517−2522.

chemical shifts.[22,28] The findings of Latil et al. in ref 28 also indicated that NMR might not be able to resolve further structural properties due to the fact that, within a given electronic class (metallic or nonmetallic), the shieldings were predicted to be approximately the same. The Knight shift contribution for metallic tubes was neglected in this study based on the assumption that metallic SWNTs with radii typically found in experiments have a low density of states at the Fermi level. Recent theoretical work has indicated that, while ultranarrow zigzag nanotubes should exhibit a Knight shift which is on the order of hundreds of parts per million, tubes wider than 1.5 nm will have a Knight shift which is inversely proportional to their diameter and relatively small (on the order of $-1$ to $-2$ ppm).[33] Moreover, the computations of Latil et al.[28] neglected terms arising from the $sp^2-sp^3$ curvature-induced rehybridization of the carbon orbitals. It was argued that these terms should be small, and therefore, the chemical shift should be roughly constant for tubes of diameters close to those typically found experimentally. An absolute value for the chemical shift with respect to a common NMR reference nucleus was not provided.

Two of us have subsequently theoretically estimated the $^{13}C$ chemical shift of the (9,0) SWNTs to be around 130 ppm.[30] From a consideration of various approximations in the DFT calculations of capped finite-sized SWNT fragments, this value was considered to be an upper bound with an estimated error of up to 5 ppm. Based on the difference between the nuclear shielding in metallic and nonmetallic SWNTs as calculated by Latil et al.,[28] we predicted a shift of around 141 ppm for metallic tubes. SWNT fragments capped with hydrogen were found to exhibit different electronic and magnetic behavior as compared to those capped with $C_{30}$.[30] The $^{13}C$ NMR chemical shifts of finite tubes terminated with fullerene hemispheres were subsequently computed at the Hartree−Fock/STO-3G level by Besley et al.[34] The resonance of the carbons in the tube (as opposed to in the cap) lay in the range of 128−138 ppm. How these results compare to those from calculations on infinite SWNTs is still unclear. For example, the longest (6,6) fragment studied by Besley et al. had a band gap of 2.67 eV, whereas isolated infinite ($n$,$n$) SWNTs are known to be metallic due to symmetry.[35]

Recently, the first DFT computations of the NMR of infinite, pristine, isolated, and bundled SWNTs have been reported in the literature.[26,27] Marques et al.[26] studied the large-gap zigzag ($n$,0) SWNTs, with $n$ ranging from 8 to 20, characterized by a "family" index $\lambda = \mathrm{mod}(n, 3) = 1$ and 2 and also reported computed magnetic susceptibilities. Our work[27] focused on all ($n$,0) SWNTs with $7 \leq n \leq 17$ and $\lambda = \mathrm{mod}(n, 3) = 0$, 1, and 2. We have shown that the results of molecular (finite-length systems calculated with an atom-centered atomic orbital basis) and periodic calculations using plane-wave basis sets can be compared directly if benzene or $C_{60}$ is chosen as the internal (computational) reference.[27] This led to the conclusion that the chemical shift of a finite (9,0) SWNT fragment converges very slowly, if at all, to the infinite limit. DFT-GIPAW calculations on infinite ($n$,0) species have demonstrated that their shifts can be fitted well by a function inversely proportional to the diameter of the tube and proportional to a constant which depends on the nanotube family.[26,27] The curvature effects on the chemical shifts for small-to-medium diameter semiconducting SWNTs led to a chemical shift range of 20 ppm for $n$ between 7 and 17, that is, the $sp^2-sp^3$ rehybridization effect is far from negligible.[27] Moreover, it was pointed out that the small-gap $\lambda = 0$ family exhibits shifts much lower than the other two families. However, it remains to be determined how to distinguish these in the experimental spectra from the $\lambda = 1$, 2 systems with a large diameter.[27]

Despite the fact that many issues still need to be resolved, theoretical work on finite and infinite pristine SWNTs has been advancing rapidly. Herein, we provide the first ab initio study of the chemical shifts of functionalized SWNTs obtained from DFT-GIPAW calculations on infinite zigzag carbon nanotubes. By virtue of the GIPAW approach, we are able to eliminate considerable uncertainties regarding the convergence behavior of the chemical shifts toward (quasi-) infinite systems that have plagued previous studies. In section 3.1, we discuss the band gaps and binding energies of the derivatized tubes. The results of the $^{13}C$ NMR calculations are presented in section 3.2. First, we examine the histograms obtained for SWNTs where NH reacts with a C−C bond parallel or diagonal to the SWNT axis. The shifts of the carbons attached to the functional group are substantially different for the two isomers, indicating that $^{13}C$ NMR could be useful in determining the site where functionalization occurs. Next, we examine the effect of decreasing the NH/C ratio when NH is attached to the parallel bond. Finally, the NMR histograms obtained for the (8,0) and (9,0) SWNTs where 2NH groups, $NCH_3$, $NCH_2OH$, and $CH_2NHCH_2$ have reacted with the parallel bond are presented. It is shown that the average chemical shift of the unfunctionalized carbons is independent of the group and that the shifts of the carbons directly attached to the group, as well as of those within the group, are independent upon the SWNT. In section 3.3, we present the $^1H$ NMR of the group−SWNT adducts. It is suggested that proton NMR may also be used to determine the site where functionalization occurs.

## 2. Methodology, Computational Details

Full geometry optimizations (all internal coordinates and cell parameters) were performed for the (7,0), (8,0), (9,0), and (10,0) pristine and functionalized SWNTs using a 2005 developer's version of the Castep code.[36,37] The starting geometries were generated by the TubeGen tool[38] using a hexagonal unit cell. Isolated pristine SWNTs were simulated in the calculations by using an intertube distance of 8 Å. To prevent intertube interactions in the functionalized systems, the intertube distances were increased by up to 9 Å, and the functional group was oriented toward the long diagonal of the unit cell. In the calculations, we have applied the Perdew−Burke−Ernzerhof (PBE) nonhybrid density functional.[39−41] A "precise" setting for the plane-wave basis with the ultrasoft pseudopotential[42] resulted in an energy

(33) Yazyev, O. V.; Helm, L. *Phys. Rev. B* **2005**, *72*, 245416-1−245416-5.
(34) Besley, N. A.; Titman, J. J.; Wright, M. D. *J. Am. Chem. Soc.* **2005**, *127*, 17948−17953.
(35) White, C. T.; Robertson, D. H.; Mintmire, J. W. *Phys. Rev. B* **1993**, *47*, 5485−5488.
(36) Segall, M. D.; Lindan, P. J. D.; Probert, M. J.; Pickard, C. J.; Hasnip, P. J.; Clark, S. J.; Payne, M. C. *J. Phys.: Condens. Matter* **2002**, *14*, 2717−2744.
(37) Clark, S. J.; Segall, M. D.; Pickard, C. J.; Hasnip, P. J.; Probert, M. J.; Refson, K.; Payne, M. C. *Z. Kristallogr.* **2005**, *220*, 567−570.
(38) Frey, J. T.; Doren, D. J. *TubeGen 3.3*; University of Delaware: Newark, DE, 2005 (web interface, http://turin.nss.udel.edu/research/tubegenonline.html).
(39) Perdew, J. P.; Burke, K.; Ernzerhof, M. *Phys. Rev. Lett.* **1996**, *77*, 3865−3868.
(40) Perdew, J. P.; Burke, K.; Ernzerhof, M. *Phys. Rev. Lett.* **1998**, *80*, 891.
(41) Hammer, B.; Hansen, L. B.; Norskov, J. K. *Phys. Rev. B* **1999**, *59*, 7413−7421.
(42) Vanderbilt, D. *Phys. Rev. B* **1990**, *41*, 7892−7895.

cutoff of about 420 eV for most of the systems considered, with the exception of the (8,0) and (9,0) $NCH_2OH$-functionalized SWNTs where a cutoff of about 588 eV was employed. The latter systems required a higher energy cutoff to achieve convergence of the calculated properties due to the hardness of the oxygen pseudopotential. Subsequently, the same computational settings were used to calculate the band structures and NMR shielding tensors of the optimized structures.

NMR shielding tensors were computed using the GIPAW method as implemented by Pickard and Mauri[43] and extended to ultrasoft pseudopotentials.[44] The shielding tensor is obtained from computations in reciprocal space and subsequent Fourier transformation to real space. The contribution from the origin of the reciprocal lattice yields a macroscopic term in the isotropic nuclear magnetic shielding. This term is given as $-(4\pi/3)\sum_{i=x,y,z}\alpha_{ii}\chi$, with $\chi$ being the macroscopic magnetic susceptibility and the $\alpha_{ii}$ being related to the shape of the sample.[45] For example, $\alpha_{xx} = \alpha_{yy} = (1/2)$ and $\alpha_{zz} = 1$ corresponds to a cylinder, whereas for a sphere, one has uniform $\alpha_{ii} = (2/3)$.[45] We have assigned values of $\alpha_{xx} = \alpha_{yy} = (1/2)$ and $\alpha_{zz} = (2/3)$, which leads to a faster convergence rate of the chemical shift with respect to the intertube distance, as was reported previously in ref 26 and was subsequently confirmed by our calculations.

All chemical shifts were determined with respect to TMS; however, for the $^{13}C$ data, benzene was used as the internal (computational) reference. It has been demonstrated that this strategy results in systematic error cancellation, yielding shifts which should be closer to those measured experimentally.[27] Thus, for the carbon shifts, we report $\delta^{TMS}_{C_6H_6}$ where

$$\delta^{TMS}_{C_6H_6}(\text{tube}) = \{\sigma(C_6H_6) - \sigma(\text{tube})\} + \delta(C_6H_6) \qquad (1)$$

$\delta(C_6H_6)$ is the experimental chemical shift of benzene with respect to TMS (126.9 ppm as quoted in ref 26), and $\sigma(C_6H_6) = 40.53$ is the calculated shielding constant for benzene. Another choice for the internal computational reference could be $C_{60}$. In ref 27, we determined that $\delta^{TMS}_{C_6H_6}(C_{60})$ is only 0.3 ppm larger than the experimental result with the aforementioned computational settings. Therefore, using $C_{60}$ instead of benzene as the internal reference will not have a substantial impact on the results. For the $^1H$ NMR, the shifts are given with respect to TMS, and an internal computational reference was not employed.

Previously, we have found that a Monkhorst−Pack *k*-point grid of dimension (1,1,*m*) with $m = 25, 20, 25$ for the (7,0), (8,0), and (10,0) pristine tubes yielded converged shielding constants.[27] SWNTs with small band gaps, such as the (9,0), displayed an oscillatory convergence behavior in the shielding constants with respect to even and odd *m*. Thus, an average obtained from odd and even *k* grids was reported. For example, for the (9,0) tube, the average of $m = 35$ and 40 was deemed to provide an appropriate estimate for the results of a fully converged calculation.[27] Within this work, most of the supercells consisted of two unit cells of the pristine SWNT and the given functional group. Hence, for the functionalized tubes, *m* was initially chosen as being approximately half as large as that for the converged pristine systems. The results were tested for convergence by increasing *m* by one. If the shielding constants from the two calculations differed by less than 0.5 ppm, we report the values obtained from the larger grid; otherwise, an average of the results from even and odd grids is given. The final values of *m* employed are listed in Table 1. The chemical shifts and band gaps for the pristine SWNTs reported here differ slightly from those published previously in ref 27 due to a different choice of the $\alpha_{ii}$ values in the macroscopic component of the isotropic nuclear magnetic shielding and the doubling of the unit cell. In most cases, the computational settings employed yield an estimated error of about 1 ppm in the $^{13}C$ NMR chemical shifts. However, the error may be slightly larger for small-gap semiconductors such as the (9,0) pristine and functionalized tubes since smaller band gaps may require a very large *k* grid so that the shieldings obtained from even and odd *m* are converged to 1 ppm.[27] For the (9,0) tube where NH was substituted at the diagonal bond, it was necessary to use an average of the results from an $m = 50$ and 51 grid to achieve reasonable convergence.

***Table 1.*** The *m* Used for the Geometry Optimizations, Band Gap, and NMR Shielding Tensor Calculations in the Monkhorst−Pack *k*-Point Grid of Dimension (1,1,*m*)[a]

| functional group | (7,0) | (8,0) | (9,0) | (10,0) |
|---|---|---|---|---|
| none (pristine SWNT) | 15 | 11 | 20/21 | 14 |
| NH | 15 | 10/11 | 20/21 | 14/15 |
| NH (site II) | 15 | 11 | 50/51 | 15 |
| NH (three unit cells) | | 8 | 15/16 | |
| NH (four unit cells) | | 6 | | |
| 2NH | | 11 | 21 | |
| $NCH_3$ | | 10/11 | 20/21 | |
| $NCH_2OH$ | | 10/11 | 20/21 | |
| $CH_2NHCH_2$ | | 10/11 | 20/21 | |

[a] Unless otherwise noted, the functional group was added to the parallel C−C bond (site I), and the supercell consisted of two unit cells of the SWNT. If two values are given, the reported chemical shifts were calculated from an average obtained from both (1,1,*m*) *k* grids. Sites I and II are illustrated in Figure 1. The geometries of the 2NH−, $NCH_3$−, $NCH_2OH$−, and $CH_2NHCH_2$−(9,0) SWNTs are shown in Figure 2.

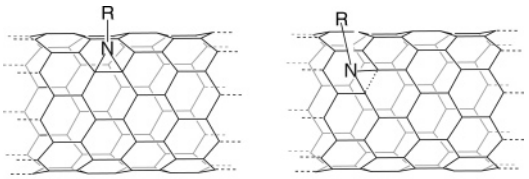


***Figure 1.*** Functionalization of a zigzag SWNT. (a) Site I: the NR group is attached to the C−C bond parallel to the tube axis. (b) Site II: the NR group substitutes into the diagonal C−C bond. The dashed lines denote a periodic system.

Geometry optimizations on TMS, benzene, NH, $NCH_3$, $NCH_2OH$, and $CH_2NHCH_2$ have been performed using cubic supercells of size 10 Å and *k* grids of (2, 2, 2), (2, 2, 2), (4, 4, 4), (4, 4, 4), (5, 5, 5), and (4, 4, 4), respectively. The plane-wave cutoffs corresponded to 490, 490, 326, 420, 588, and 420 eV for the aforementioned molecules. The shielding tensors for TMS and benzene have been computed using identical settings. To calculate binding energies, spin-polarized calculations were performed on open-shell triplet configurations of the isolated functional groups, as in ref 46.

## 3. Results and Discussion

We have considered functionalization of a range of zigzag SWNTs with the functional groups NH, $NCH_3$, $NCH_2OH$, and $CH_2NHCH_2$ and different binding modes, as shown in Figures 1 and 2. The first three groups have been selected as models for amine-terminated poly(ethylene glycol) (PEG), which is frequently used as a polar functional group for studies of SWNTs in solution. In other functionalization processes, a five-membered *N*-heterocycle containing two SWNT carbons is obtained instead.[11−13,47] The different models for the N-terminated PEG systems allow verification if the addition of electron-donating or -withdrawing groups at the nitrogen has

(43) Pickard, C. J.; Mauri, F. *Phys. Rev. B* **2001**, *63*, 245101-1−245101-13.
(44) Yates, J. First Principles Calculation of Magnetic Resonance. Ph.D. Thesis, University of Cambridge, Cambridge, U.K., 2003.
(45) Mauri, F.; Pfrommer, B. G.; Louie, S. G. *Phys. Rev. Lett.* **1996**, *77*, 5300−5303.
(46) Zheng, G. S.; Wang, Z.; Irle, S.; Morokuma, K. *J. Am. Chem. Soc.* **2006**, *128*, 15117−15126.
(47) Yao, Z. L.; Braidy, N.; Botton, G. A.; Adronov, A. *J. Am. Chem. Soc.* **2003**, *125*, 16015−16024.

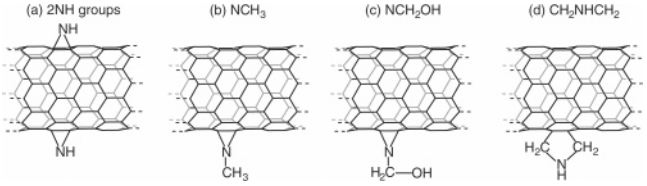


***Figure 2.*** Different modes of SWNT functionalization considered in this work: (a) two NH groups, (b) a single $NCH_3$ group, (c) a single $NCH_2OH$ group, and (d) a single $CH_2NHCH_2$ group. The supercells contained two units cells of the (8,0) or (9,0) tubes. The functional groups were added to the C−C bond parallel to the tube axis (site I), as shown here. For the NH group, substitution into a diagonal bond (site II), as shown in Figure 1, was also considered. The dashed lines denote a periodic system.

any profound impact on the chemical shifts of the SWNT carbons. In the following sections, it will be shown that this is not the case, at least for addition to the parallel C−C bond. Therefore, each of these three functional groups can be considered a reasonable model for the N-terminated PEG chain. Based on these results, it is unlikely that substitution of the amine hydrogen in the $CH_2NHCH_2$ groups yields drastically different NMR data.

**3.1. Bonding Energies and Band Gaps.** A functional group may react with either a C−C bond parallel (site I) or diagonal (site II) to the axis of a zigzag SWNT. The former are always shorter than the latter; however, as the radius of the tube increases, the difference between the bond lengths decreases.[48] The parallel and diagonal bonds have more double- and single-bond character, respectively. Figure 1 sketches the functionalization at each site. A reaction with the parallel bond yields a three-membered ring due to the addition of N−R to the C−C double bond. In this case, the carbons attached to NH formally change their hybridization from $sp^2$ to $sp^3$. Alternatively, the group may react with site II, breaking the diagonal C−C bond. Here, the substituted carbons remain formally $sp^2$-hybridized. For example, upon formation of the (8,0)−NH adduct, the C−C bond elongates from 1.418 to 1.495 Å (site I) and from 1.434 to 2.418 Å (site II). Geometry optimizations for NH-functionalized (7,0), (8,0), (9,0), and (10,0) SWNTs have been performed in this work, and both sites have been considered. The NH/C ratios were 1.79, 1.56, 1.39, and 1.25%, respectively, due to the varying amount of carbons in the supercells. In accordance with other calculations,[14,15] the structures where NH was attached to the diagonal bond were found to be 7.64, 6.54, 4.24, and 7.18 kcal/mol lower in energy for the aforementioned tubes, respectively (Table 2). Other studies have indicated that addition to the parallel bond is favored instead and that the energy difference between the two isomers decreases with increasing radius of the tube.[16] The energy differences which we calculate are not negligible but only indicate thermodynamic stability. To our knowledge, the corresponding reaction barriers have not yet been calculated, and therefore, the kinetic parameters are unknown. However, one might expect that breaking the diagonal bond would have a higher barrier because of significant elongation along the reaction coordinate, in accordance with the principle of least motion.[49]

For all of the nanotubes considered, the reaction with NH was calculated as being very exothermic, although one needs to keep in mind that the formation of the NH species itself requires a significant amount of energy. The binding energies are known to be larger for metallic and small-gap semiconducting SWNTs such as the (9,0) than for semiconducting tubes such as the (10,0).[14] At the same time, the curvature-induced strain of the smaller tubes increases their reactivity. These two factors explain the trend for the calculated magnitudes of the binding energies: (7,0) > (8,0) ≈ (9,0) > (10,0).

In order to investigate the effect of the degree of functionalization, calculations have been performed on (8,0) and (9,0) SWNTs derivatized by 2NH groups, as shown in Figure 2a (3.13 and 2.78% NH/C ratio). Supercells containing three and four unit cells of the pristine tubes have also been optimized. The magnitude of the binding energy per NH unit increased slightly as the NH/C ratio increased, in contrast to the findings reported in ref 14. However, these authors only considered geometries where the functional group reacted with the diagonal C−C bond. Our results do not necessarily imply that further addition of NH will follow the same trend. Instead, it is conceivable that, past a critical degree of functionalization, the magnitude of the binding energy per NH group will decrease. The addition of $NCH_3$, $NCH_2OH$, and $CH_2NHCH_2$ to the parallel C−C bonds in (8,0) and (9,0) nanotubes was also investigated. Figure 2b−d shows geometries of these species. In all cases, the binding energies for the (8,0) adducts were slightly lower than those for the (9,0). The relative order of exothermicities was found to be $CH_2NHCH_2$ > NH (site II) > $NCH_2OH$ > NH (site I) > $NCH_3$.

Examination of Table 3 reveals that the band gaps of the derivatized tubes are strongly dependent upon the bond which is functionalized, resulting in differences of up to 0.48 eV between the two (10,0)−NH adducts. For a given site and degree of functionalization, the band gaps are almost independent of the group, within the margin of error of our calculations. This

***Table 2.*** Calculated Binding Energies[a] for Functionalized SWNTs[b] in kcal/mol

| functional group | (7,0) | (8,0) | (9,0) | (10,0) |
|---|---|---|---|---|
| NH | −54.85 | −49.28 | −49.32 | −43.01 |
| NH (site II) | −62.49 | −55.82 | −53.56 | −50.19 |
| NH (three unit cells) | | −46.68 | −46.91 | |
| NH (four unit cells) | | −45.34 | | |
| 2NH | | −101.27 | −99.86 | |
| $NCH_3$ | | −32.87 | −32.73 | |
| $NCH_2OH$ | | −53.06 | −49.50 | |
| $CH_2NHCH_2$ | | −63.05 | −58.88 | |

[a] For the functional group X, the binding energy is given as BE(X−SWNT) = $E$(X−SWNT) − $E$(X) − $E$(SWNT). [b] Unless otherwise noted, the functional group was added to the parallel C−C bond (site I), and the supercell consisted of two unit cells of the SWNT.

***Table 3.*** Unscaled Calculated Band Gaps for Functionalized SWNTs[a] in eV

| functional group | (7,0) | (8,0) | (9,0) | (10,0) |
|---|---|---|---|---|
| none (pristine SWNT) | 0.200 | 0.575 | 0.102 | 0.747 |
| NH | 0.315 | 0.432 | 0.074 | 0.197 |
| NH (site II) | 0.220 | 0.569 | 0.015 | 0.673 |
| NH (three unit cells) | | 0.459 | 0.084 | |
| NH (four unit cells) | | 0.487 | | |
| 2NH | | 0.260 | 0.779 | |
| $NCH_3$ | | 0.422 | 0.074 | |
| $NCH_2OH$ | | 0.425 | 0.067 | |
| $CH_2NHCH_2$ | | 0.436 | 0.040 | |

[a] Unless otherwise noted, the functional group was added to the parallel C−C bond (site I), and the supercell consisted of two unit cells of the SWNT.

(48) Sun, G. Y.; Kürti, J.; Kertesz, M.; Baughman, R. H. *J. Phys. Chem. B* **2003**, *107*, 6924−6931.
(49) Rice, F. O.; Teller, E. *J. Chem. Phys.* **1938**, *6*, 489−496.

is in agreement with the findings of refs 50 and 51. For the (8,0) and (9,0) SWNTs where the group has been added to the parallel bond, the band gaps vary between 0.422 and 0.436 eV and between 0.040 and 0.074 eV, respectively. It appears that the band gaps are relatively insensitive to the chemical nature of the group but sensitive to the hybridization of the carbons directly linked to it. In fact, for the (7,0), (8,0), and (10,0) NH-functionalized systems, the gaps are closer to those of the pristine species when substitution at the diagonal, as opposed to addition to the parallel C−C bond, takes place. Thus, for effective band-gap engineering, it would be important to determine which site is functionalized. For the (8,0) and (9,0) SWNTs where NH has reacted with the parallel bond, decreasing the degree of functionalization results in a tendency of the gap to approach that of the pristine species, in accordance with the results of Zhao et al.[14] Interestingly, the addition of two NH groups, as shown in Figure 2a, changes the band gap considerably. In comparison to the pristine tube, the gap increases by 0.677 eV and decreases by 0.315 eV for the (9,0) and (8,0) systems, respectively.

**3.2. The $^{13}C$ NMR Chemical Shifts of Functionalized SWNTs.** Histograms of the $^{13}C$ NMR chemical shifts where an NH group has been added to the parallel C−C bond (site I functionalization) are shown in Figure 3. The small peak at around 44 ppm is due to the $sp^3$ carbons which are directly attached to the functional group. Interestingly, this shift is rather independent of the nanotube diameter, varying by less than 3 ppm. It is comparable to a shift of 43.7 ppm for 2,3-*trans*-diphenylaziridine and of a 43.8 ppm shift for aziridine trisubstituted with methyl and two phenyl groups trans to each other.[52] Thus, the shifts of these carbons are typical for those in aziridine substituted with aromatic groups. Substantial broadening of the peak arising from the underivatized SWNT carbons occurs as a result of functionalization. Whereas all of the carbon shifts in the pristine species were essentially the same, they now vary by 7−21 ppm within a given NH−SWNT adduct. For the (7,0)−, (8,0)−, and (10,0)−NH adducts, the average shift of the unfunctionalized carbons is somewhat below that of the carbons in the corresponding pristine tubes. For the (9,0) species, the average shift is 2.5 ppm higher. It is, as of yet, unclear why the average shift of the members of the $\lambda = 1, 2$ families decreases, whereas for the small-gap (9,0) system, it increases upon functionalization. More detailed investigations are required to analyze this behavior and to confirm that the direction of the shift change upon functionalization can be attributed to the SWNT family. It is clear that the functionalization yields a significantly broadened NMR signal as compared to what would be obtained for a system of isolated pristine SWNTs. (In the figures, the range of chemical shifts near the base of the peaks is indicated.) For the range of SWNTs considered here, the direction of the shift change (negative for the $\lambda = 1, 2$ family SWNTs and positive for the $\lambda = 0$ (9,0) SWNT) indicates that, for a heterogeneous sample containing these functionalized SWNTs, the average of the NMR peaks from individual members of the sample should lie closer together than those for a sample of pristine SWNTs. However, experimental uncertainties of a few parts per million are not uncommon due to the broadness of the signals, and it is unclear if sufficient resolution may be obtained to observe the shift change upon functionalization.

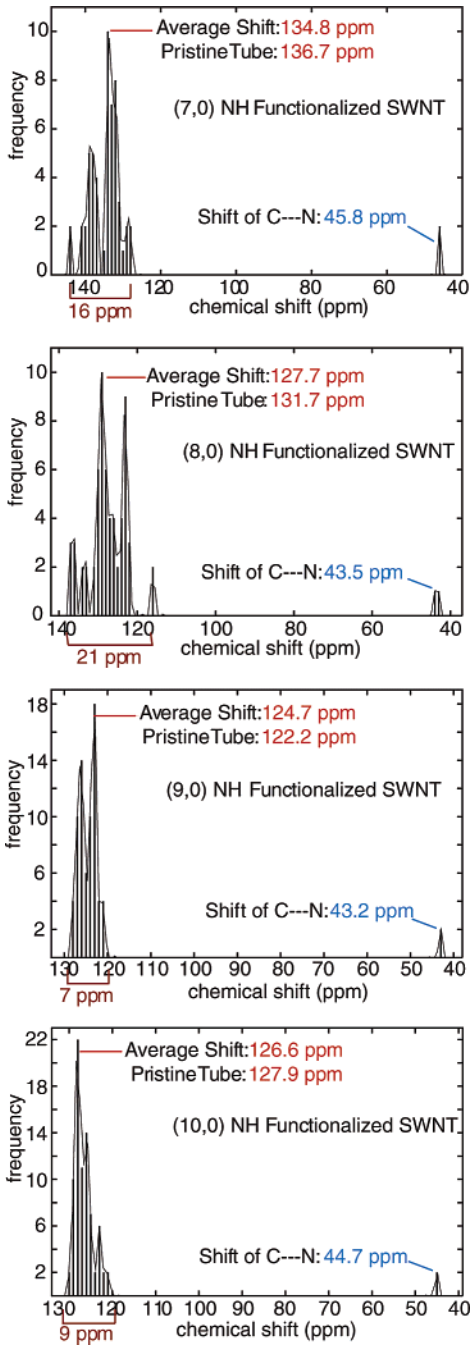


***Figure 3.*** Calculated histograms of the $^{13}C$ NMR chemical shifts of NH-functionalized (7,0), (8,0), (9,0), and (10,0) SWNTs. The supercell consisted of two unit cells of the zigzag tube and a single NH group. The functional group was attached to the C−C bond parallel to the tube axis (site I).

The optimized structures of the functionalized SWNTs exhibit, in all cases, a pronounced "ovality" perpendicular to the tube axis. This is clearly seen in the cross section of the optimized (8,0) systems shown as an example in Figure 4. One may expect that this geometry change leads to a noticeable broadening of the NMR signal from the unsubstituted SWNT carbons. In order to investigate this issue further, we have performed an NMR computation using the oval geometry of

(50) Lee, Y.-S.; Nardelli, M. B.; Marzari, N. *Phys. Rev. Lett.* **2005**, *95*, 076804-1−076804-4.
(51) Zhao, J. J.; Park, H. K.; Han, J.; Lu, J. P. *J. Phys. Chem. B* **2004**, *108*, 4227−4230.
(52) Mison, P.; Chaabouni, R.; Diab, Y.; Martino, R.; Lopez, A.; Lattes, A.; Wehrli, F. W.; Wirthlin, T. *Org. Magn. Reson.* **1976**, *8*, 79−89.

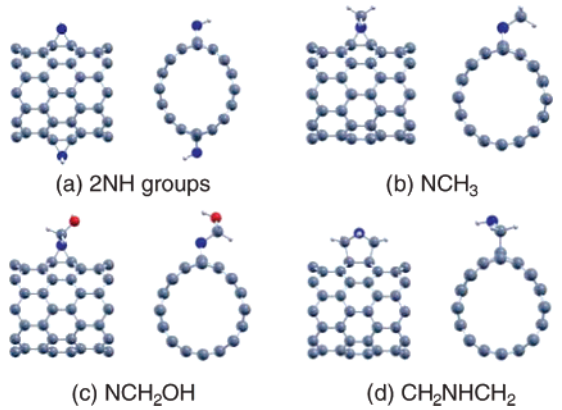


***Figure 4.*** Optimized structures of an (8,0) SWNT with site I functionalization. (a−d) Labeling as in Figure 2.

the optimized NH−functionalized (8,0) SWNT but without the NH group attached. The average shift of the carbons (not including those that are directly bound to the NH group) was 131.0 ppm, with a similarly pronounced width of the NMR peak in the histogram (not shown) as that for the functionalized (8,0) SWNT shown in Figure 3. The difference in the average shift is mainly due to the contributions from the carbons in the vicinity of the functional group, which become significantly less shielded when the NH group is removed. The functionalized carbons of the (8,0) system have a computed shift of 43.5 ppm, as shown in Figure 3. A shift of 172 ppm is obtained instead for these carbons upon removal of the functional group. Obviously, the NMR shifts of the functionalized carbons are strongly effected both by the geometry change (leading to a substantial deshielding) and by the electronic effects due to their binding to the functional group, which overcompensates the geometry-induced deshielding. Further inspection of the data revealed that the geometry difference (functionalized versus pristine SWNT) mainly affects the carbons far away from the group, whereas the electronic effects from the functional group strongly influence the chemical shift of carbons in the vicinity of the functional group (and, of course, the shift of the carbons directly bound to it); however, the latter effect decays quite rapidly with distance.

Figure 5 displays $^{13}$C NMR histograms of the SWNTs where NH is added into the diagonal C−C bond (site II functionalization). In this case, the shifts of the substituted carbons do not differ substantially from those of the rest of the carbons in the tube since they remain sp$^2$-hybridized. For the (7,0), (8,0), (9,0), and (10,0) adducts, they are located at 115.0, 111.5, 140.5, and 104.2 ppm, respectively. In contrast to the behavior found for site I functionalization, the results for site II show that the shifts of the functionalized carbons are highly dependent upon the SWNT structure to which NH binds. This suggests that it may be possible to determine by NMR if a diagonal or parallel C−C bond is functionalized. With the exception of the (9,0) tube, the shifts of the carbons attached to the group are slightly lowered after functionalization. This is in agreement with Cahill et al.,[23] who found that the peak attributed to these carbons moved from ∼120 to ∼118 ppm upon reaction with phenol. Whereas Cahill et al. attributed this behavior to a change in hybridization from sp$^2$ to sp$^3$, our results suggest that shifts of this magnitude should correspond to sp$^2$ carbons. However, it still remains to be seen if results obtained for infinite SWNTs

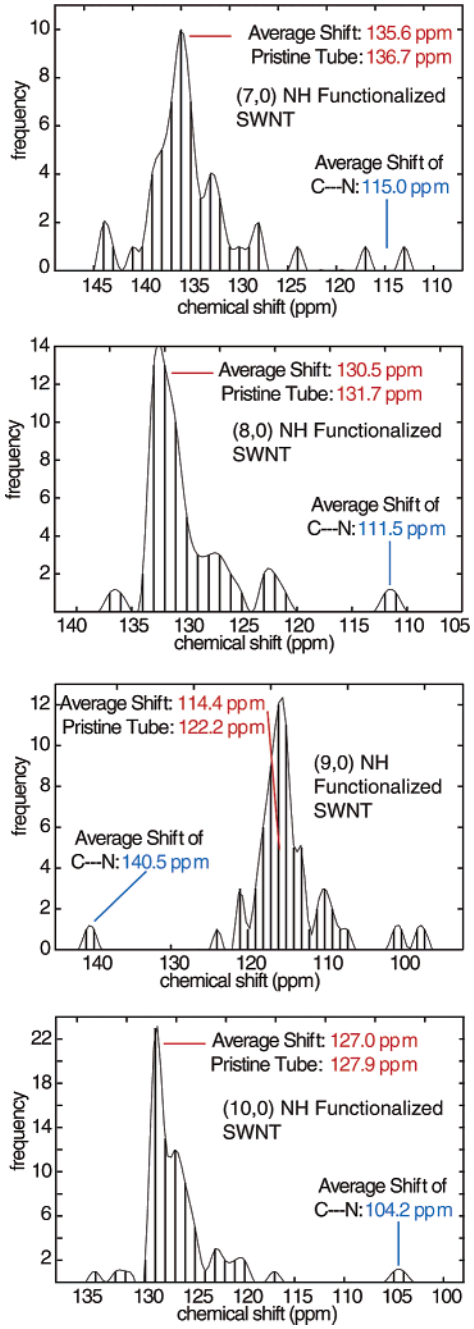


***Figure 5.*** Calculated histograms of the $^{13}$C NMR chemical shifts of NH-functionalized (7,0), (8,0), (9,0), and (10,0) SWNTs. The supercell consisted of two unit cells of the zigzag tube and a single NH group. The functional group was attached to the C−C bond diagonal to the tube axis (site II).

are transferable to shortened, uncapped SWNTs. For the tubes belonging to the $\lambda = 1, 2$ families, the shifts of the substituted carbons decrease as the radius of the tubes increases. On the other hand, for the small-gap (9,0) system, they are higher than those corresponding to the unfunctionalized carbons. Therefore, it might be possible to identify the composition of a sample by monitoring the signals arising from the carbons that are directly attacked in the functionalization process, provided that functionalization occurs at one of the diagonal bonds. It would be interesting to compute the shifts of larger tubes to determine if a trend exists; however, due to the excessive computational cost involved, this is beyond the scope of the work presented here. For the SWNTs belonging to the $\lambda = 1, 2$ families, the average

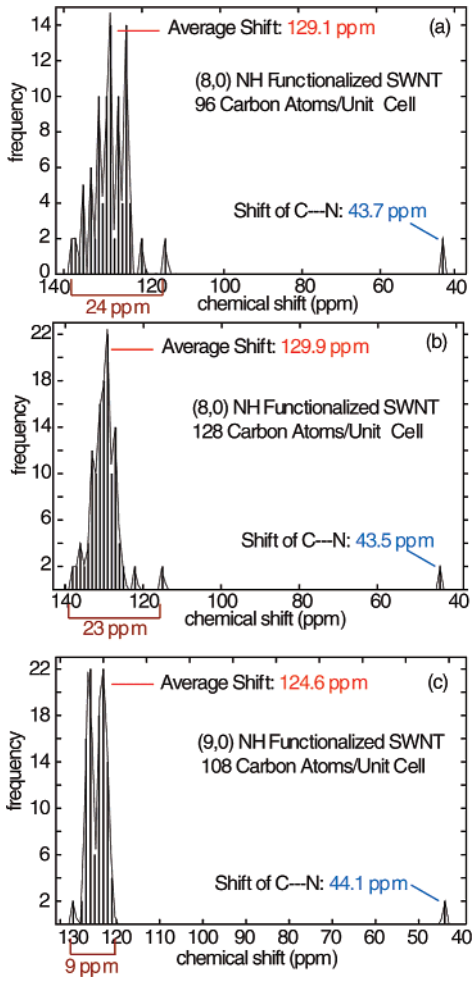


***Figure 6.*** Calculated histograms of the $^{13}C$ NMR chemical shifts of NH-functionalized SWNTs. The functional group was attached to the C−C bond parallel to the tube axis (site I). The supercell consisted of a single NH group and (a) three unit cells of an (8,0) tube, (b) four unit cells of an (8,0) tube, and (c) three unit cells of a (9,0) tube.

shifts of the underivatized carbons decreased slightly as compared to those of the pristine tube but to a lesser extent than when the parallel C−C bond was functionalized with NH. The (9,0) system belonging to the $\lambda = 0$ family behaves differently and affords a significantly lower average shift for the underivatized carbons in the tube. Again, this behavior hints at a possibility of identifying SWNTs of this family, possibly by monitoring the chemical shift change upon functionalization. Also, the computed results indicate that a pronounced site II preference of the functional group would result in an overall stronger peak broadening of a heterogeneous sample than for site I functionalization. The average shifts of the $\lambda = 0$ and 1, 2 SWNT family members separate upon site II functionalization, whereas for site I functionalization, the average shifts of the $\lambda = 0$ and 1, 2 members are separated less than those of the pristine SWNTs.

The question arises how the degree of functionalization affects the $^{13}C$ NMR chemical shifts. To this end, computations with one functional group per unit cell and varying sizes of the unit cells were performed, leading to varying ratios of functionalized to unfunctionalized SWNT carbons. The (8,0) and (9,0) tubes with NH attached to the parallel C−C bond (site I) have been considered as examples. The results are shown in Figure 6. Comparison of Figures 6 and 3 reveals that the shifts of the carbons directly bound to the group are quite insensitive to the NH/C ratio. This is in line with our finding that, for site I, the $^{13}C$ shifts of the functionalized carbons appear to be rather insensitive to the SWNT electronic structure as a function of the tube radius. Therefore, our computational data support the findings of Zhao et al.[51] who suggested that the functionalized site can be viewed as a local $sp^3$ defect. For the (8,0) system, the average shift of the underivatized carbons approaches that of the pristine tube as the degree of functionalization decreases. With increasing supercell size, the band gaps also approach that of the pristine tubes. The histograms show that the simulated NMR peaks become smoother with increasing C/NH ratio. At the same time, the histogram widths at half peak height and at the base remain roughly the same as the C/NH ratio increases. Therefore, for the unit cell sizes that we were able to consider in this study, a noticeable NMR peak broadening remains at all degrees of functionalization, and it is apparent that the $sp^3$ defect has a considerable effect on the nanotube NMR in terms of peak width.

In order to determine how chemical differences in the functional group influence the nanotube chemical shifts, calculations were performed with $NCH_3$, $NCH_2OH$, and $CH_2NHCH_2$ attached to the parallel bond in (8,0) and (9,0) SWNTs (see Figure 2). The NMR histograms in Figures 3, 7, and 8 reveal that, within the estimated error of the computations, the average shift of the underivatized SWNT carbons is insensitive of the substituent R at the N−R group. For the (8,0) and (9,0) systems with one group per double unit cell, the average varies between 127.7 and 128.8 ppm and between 123.4 and 124.7 ppm, respectively. In section 3.1, it was pointed out that the band gaps of these functionalized SWNTs are also nearly identical. We, therefore, suggest that the functional groups as studied here are suitable models for PEG−N-functionalized nanotubes. Interestingly, the average chemical shifts for the $CH_2NHCH_2$ functional group are also quite similar to those obtained for the systems used to model PEG−N-functionalized nanotubes. In general, the shift broadening of the $sp^2$ carbons does not vary greatly for the different groups considered. The four outlying shifts at about 140 ppm in Figure 8d for the (9,0)−$CH_2NHCH_2$ system increase the broadening by approximately 10 ppm. They originate from SWNT carbons in the direct vicinity of the functionalized carbon atoms. In the future, the development of new analysis tools will help us to determine why the broadening is much larger in this particular case. For the site-I NH-functionalized SWNTs, it was previously noted that the shifts of the derivatized carbons varied by only 2.6 ppm for all of the tubes considered. Examination of Figures 7 and 8 also indicates that these shifts are rather insensitive to the SWNT radius. For $NCH_3$ and $NCH_2OH$, they are located at 47.5/47.2 and 47.0/46.8 ppm for the (8,0) and (9,0) systems, respectively. For $CH_2NHCH_2$, the agreement is not quite as close. These shifts are found at 49.9 and 45.8 ppm, respectively. A similar behavior is observed for the shifts of the carbons within the functional group. For example, the $NCH_3$ carbons yield a shift of 29.8 and 30.2 ppm for the functionalized (9,0) and (8,0) SWNTs. These shifts are comparable to a shift of 28.3 ppm for methylamine.[53] Those carbons comprising the $CH_2NHCH_2$ group exhibit a shift of 76.4 ppm in both SWNTs (note that

(53) Eggert, H.; Djerassi, C. *J. Am. Chem. Soc.* **1973**, *95*, 3710−3718.

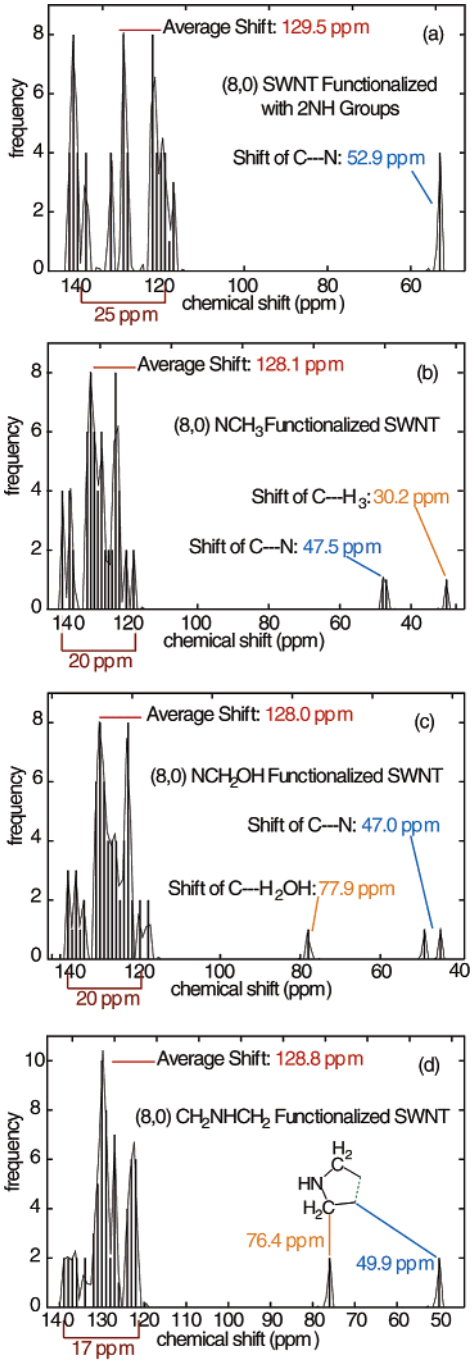


***Figure 7.*** Calculated histograms of the $^{13}C$ NMR chemical shifts of (8,0) SWNTs functionalized with (a) two NH groups, (b) a single $NCH_3$ group, (c) a single $NCH_2OH$ group, and (d) a single $CH_2NHCH_2$ group. The supercell consisted of two units cells of the (8,0) tube, and the functional group was attached to the C−C bond parallel to the tube axis (site I).

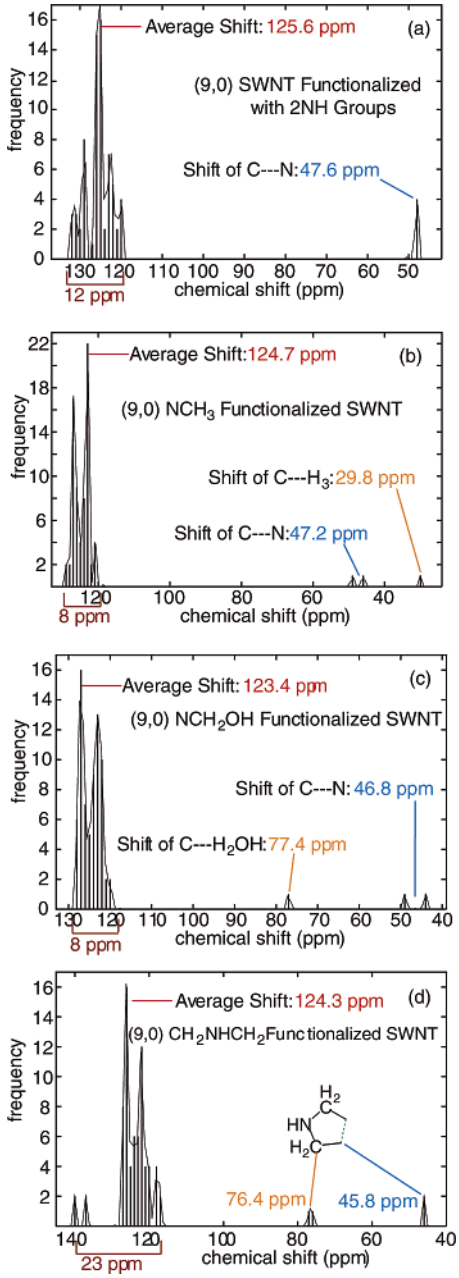


***Figure 8.*** Calculated histograms of the $^{13}C$ NMR chemical shifts of (9,0) SWNTs functionalized with (a) two NH groups, (b) a single $NCH_3$ group, (c) a single $NCH_2OH$ group, and (d) a single $CH_2NHCH_2$ group. The supercell consisted of two units cells of the (9,0) tube, and the functional group was attached to the C−C bond parallel to the tube axis (site I).

this shift differs substantially from the 47.1 ppm obtained for the carbons directly attached to nitrogen in pyrrolidine[54]). Finally, the shifts of the $NCH_2OH$ carbons in the (8,0) and (9,0) systems are 77.9 and 77.4 ppm, differing by only 0.5 ppm.

Comparison of Figure 3 with Figures 7a and 8a shows that addition of a second NH group raises the average chemical shift of the underivatized carbons by about 1−2 ppm, and the peak width is slightly broadened. Moreover, as Table 3 shows, the additional NH group significantly changes the band gap. Upon the second functionalization, the shifts of the $sp^3$ carbons also increase by 9.4 and 4.4 ppm for the (8,0) and (9,0) SWNTs, respectively. They are comparable to shifts of 54.9 and 47.9 ppm for aziridine trisubstituted with methyl, phenyl, and ethyl or two phenyl and one isopropyl group.[52] Thus, the variations found here for the shifts of the substituted SWNT carbons are in line with variations of the $^{13}C$ shifts of aziridine derivatives containing aromatic groups. This indicates that the reaction of the SWNT−NH adduct with a second NH, yielding a geometry such as that shown in Figure 2a, affects the electronic and magnetic structure of the tubes significantly. Subsequent studies need to determine if the functional groups in such systems can still be viewed in terms of a localized $sp^3$ defect.

(54) Berger, S.; Braun, S.; Kalinowski, H. O. *$^{13}C$ NMR Spektroskopie*; Thieme Verlag: New York, 1984.

***Table 4.*** Calculated $^1H$ NMR Chemical Shifts of Functionalized SWNTs[a] in ppm[b]

| functional group | (7,0) | (8,0) | (9,0) | (10,0) |
|---|---|---|---|---|
| NH | 2.05 | −0.29 | 0.91 | 1.31 |
| NH (site II) | 6.02 | 5.21 | −.50 | 5.40 |
| NH (three unit cells) | | −1.04 | 0.53 | |
| NH (four unit cells) | | −1.17 | | |
| 2NH | | 4.24 | 2.48 | |
| $NCH_3$ | | 3.25 | 3.88 | |
| $NCH_2^*OH$[c] | | 5.15 | 6.20 | |
| $NCH_2OH^*$[c] | | 0.62 | 0.93 | |
| $CH_2^*NHCH_2^*$[c] | | 5.78 | 6.34 | |
| $CH_2NH^*CH_2$[c] | | 2.01 | 2.44 | |

[a] Unless otherwise noted, the functional group was added to the parallel C−C bond (site I), and the supercell consisted of two unit cells of the SWNT. [b] NMR reference: TMS. [c] Asterisk denotes the hydrogen(s) for which the shift, or shift average, is given.

**3.3. The $^1H$ NMR Chemical Shifts of Functionalized SWNTs.** The proton chemical shifts calculated for the derivatized SWNTs are given in Table 4. The first two rows suggest that $^1H$ NMR may also be useful in determining which bond is functionalized. Except for the (9,0), which behaves differently yet again, the adducts where NH is added to the parallel bond yield shifts which are consistently lower by between 4.0 and 5.5 ppm than those where substitution at the diagonal bond occurs. It is likely that the hybridization of the nitrogen plays a role here. The optimized C−N−C angles for site I functionalization (yielding the aziridine moiety) are 60° for all of the SWNTs considered in this study; whereas for site II functionalization, the angles are between 96 and 98°. For both the (8,0) and (9,0) tubes, the proton shifts decrease with decreasing degree of functionalization. This trend might indicate an increasingly strong ring-current influence from the decreasingly perturbed SWNT. This is in contrast to the shifts of the derivatized carbons which are located at around 44 ppm for site-I functionalization, independent of the NH/C ratio as was noted in the previous section. The addition of a second NH group per double unit cell was found to change the band gap and shifts of the derivatized carbons considerably. Comparison of the first and fifth rows in Table 4 illustrates that this addition also causes the proton shift to increase substantially. The $^1H$ shifts of a given functional group appear to be somewhat higher, by 0.3−1.2 ppm, for the (9,0) than those for the (8,0) systems. This is also in contrast to the finding that the $^{13}C$ shifts within the functional group were independent of the SWNT for site I.

## 4. Conclusions

The computational results presented in this work indicate that NMR spectroscopy may provide a wealth of information on the functionalization of carbon nanotubes. The functionalization was found to be responsible for a significant line broadening of the NMR signals of the SWNT carbons. A large portion of this broadening can be traced back to the geometrical distortion of the SWNT upon functionalization. However, the average shift of the unfunctionalized SWNT carbons was found to be quite similar to the shifts calculated for the pristine SWNTs. Therefore, it is not surprising that experiments performed on functionalized soluble SWNTs have located a broad NMR signal at approximately the same shift range as that calculated for pristine SWNTs. It was shown that a substantial NMR peak broadening for each SWNT structure occurs over a wide degree of functionalization (ratio of functional group to total number of carbons in the SWNT). The trends of the shifts of the carbons directly bound to the functional group strongly depend on the functionalization site (parallel or diagonal C−C bond in zigzag tubes). For the former, they are independent; whereas for the latter, they are dependent on the SWNT radius. For site II functionalization, a comparison of the (9,0) SWNT with the other systems suggests that there might also be a pronounced SWNT−family trend observed in these shifts. Therefore, this information may ultimately be a useful guide to determine experimentally, with the help of NMR techniques, if there is a strong site preference for a functional group in a sample of carbon nanotubes or, perhaps, even yield information regarding the composition of a sample's diameter distribution and content of various SWNTs or SWNT families.

**Acknowledgment.** We would like to thank an undergraduate student, Brian Walczak, for performing some of the computations. J.A. acknowledges support from the Center of Computational Research at SUNY Buffalo and is grateful for financial support from the CAREER program of the National Science Foundation (Grant No. CHE−0447321). E.Z. acknowledges financial support from the "International Max-Planck Research School for Advanced Materials" (IMPRS-AM). C.J.P. is supported by an EPSRC Advanced Research Fellowship.

**Supporting Information Available:** Lattice parameters, fractional coordinates, and energies of pristine and functionalized SWNTs, functional groups, benzene, and TMS optimized with Castep (PBE functional). This material is available free of charge via the Internet at http://pubs.acs.org.

JA069110H